Effects of Inorganic and Organic Salts on Aggregation Behavior of Cationic Gemini Surfactants

Defeng Yu,[†] Xu Huang,[†] Manli Deng,[†] Yiyang Lin,[‡] Lingxiang Jiang,[‡] Jianbin Huang,*[,‡] and Yilin Wang*[,†]

Beijing National Laboratory for Molecular Sciences (BNLMS), Key Laboratory of Colloid and Interface Science, Institute of Chemistry, Chinese Academy of Sciences, China, and College of Chemistry and Molecular Engineering, Peking University, Beijing 100190, People's Republic of China

Received: June 30, 2010; Revised Manuscript Received: October 8, 2010

All salts studied effectively reduce critical micelle concentration (CMC) values of the cationic gemini surfactants. The ability to promote the surfactant aggregation decreases in the order of C_6H_5COONa > *p*-$C_6H_4(COONa)_2$ > Na_2SO_4> NaCl. Moreover, only C_6H_5COONa distinctly reduces both the CMC values and the surface tension at CMC. For 12-4-12 solution, the penetration of $C_6H_5COO^-$ anions and charge neutralization induce a morphology change from micelles to vesicles, whereas the other salts only slightly increase the sizes of micelles. The 12-4$(OH)_2$-12 solution changes from the micelle/vesicle coexistence to vesicles with the addition of C_6H_5COONa, whereas the other salts transfer the 12-4$(OH)_2$-12 solution from the micelle/vesicle coexistence to micelles. As compared with 12-4-12, the two hydroxyls in the spacer of 12-4$(OH)_2$-12 promote the micellization of 12-4$(OH)_2$-12 and reduce the amounts of C_6H_5COONa required to induce the micelle-to-vesicle transition.

Introduction

Effects of salts on aggregation behaviors of ionic surfactants in aqueous solutions are vital to many applications for detergency and emulsification in industry. When surfactant and salt are mixed in solution, salting-out phenomenon often happens.[1−3] According to hydration theory,[4] salting-out is the result of preferential movement of water molecules, which immobilize and quench their role as solvents, from coordination shells of surfactant molecules to those of salts. The effects of halide salts on the growth of micelles in ionic surfactant solutions have been systematically studied.[5,6] With the addition of inorganic salts, the reduced electrostatic repulsion among the surfactant headgroups is a key factor to influence the morphology of aggregates in ionic surfactant solutions. For conventional single-chain cationic surfactants, micelles may change from global to rodlike or wormlike with the addition of inorganic salts.[7,8] Organic salts including salicylate[9−11] and tosilate[12] with an aromatic phenyl group, so-called hydrotropes, have also been studied in ionic surfactant systems. Compared with inorganic salts, most organic salts have additional hydrophobic interaction with ionic surfactants in aqueous solutions besides electrostatic interaction.[13] Benzene rings in organic salts may penetrate into micelles, inducing strong hydrophobic interaction, reducing electrostatic repulsion between the hydrophilic headgroups, and finally leading to tight packing and possible reduced curvature of surfactant aggregates.[14] Therefore, wormlike micelles were often observed when organic salts were added to ionic surfactant solutions.[15−21] In addition, the refined structures of organic salts may affect their adsorption on the surface of aggregates.[22] The position of substituent on the benzene ring of organic salt directly determines how hydrophobic interaction between organic salts and surfactant aggregates works.[13] Therefore, the position of substituent on the benzene ring of organic salt may influence the morphology of surfactant aggregates. Obviously, organic and inorganic salts affect the aggregation of surfactants in quite different ways.

In recent years, gemini surfactants have attracted great attention as a new type of surfactants. Compared with conventional single-chain surfactants, gemini surfactants have high surface activity, low critical micelle concentrations (CMCs), and unusual aggregation morphologies.[23−25] As previously reported, cationic gemini surfactants 12-*s*-12 ($s = 2, 3$) can form wormlike micelles, whereas 12-4-12 forms only spherical micelles.[26] Vesicles, bilayer fragments, and even wormlike micelles were found in 16-3-16 solutions.[27] Moreover, the morphology changes in gemini surfactant solutions can be controlled by the addition of salts.[3,28−31] For inorganic salts, it has been reported that a transition from small vesicles to giant vesicles occurred in cationic gemini surfactant solution at proper NaCl concentration and specific temperature.[28] Upon the addition of organic salts, vesicles were formed with the addition of methyl orange and sodium salicylate in some ionic surfactant solutions.[29,32] Even twisted membranes were found in hydrogels consisting of cationic gemini surfactant and organic salt.[33−35] However, the differences between the interactions of inorganic and organic salts with cationic gemini surfactants have not yet been reported systematically up to date.

In the present work, effects of inorganic and organic salts on the aggregation behavior of cationic gemini surfactants 1,4-bis(*N*-dodecyl-*N*,*N*-dimethylammonium)-butane dibromide (12-4-12) and 2,3-dihydroxyl −1,4-bis(*N*-dodecyl-*N*,*N*-dimethylammonium)-butane dibromide (12-4$(OH)_2$-12) (Figure 1), which have different spacer groups, have been investigated. The cationic gemini surfactants have two charged headgroups connected by a hydrophobic or a hydrophilic spacer, respectively. On the basis of this structure, divalent anions may have special binding with the headgroups of cationic gemini surfac-

* To whom correspondence should be addressed. E-mail: yilinwang@iccas.ac.cn (Y.W.), JBHuang@pku.edu.cn (J.H.).
[†] Chinese Academy of Sciences.
[‡] Peking University.

10.1021/jp106031d
Published on Web 10/28/2010

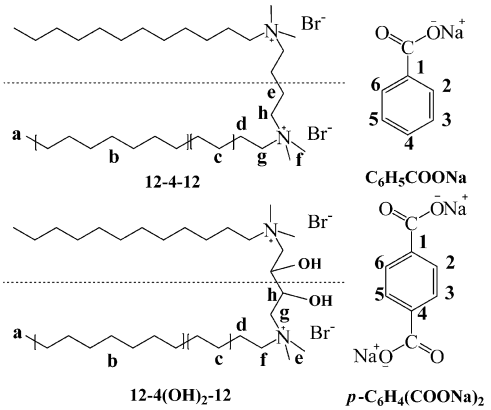

Figure 1. Chemical structures and ^{1}H NMR signal assignments of cationic gemini surfactants 12-4-12 and 12-4(OH)$_2$-12 and organic salts C_6H_5COONa and p-$C_6H_4(COONa)_2$.

tants. Therefore, NaCl and Na_2SO_4 are chosen as representative inorganic salts, whereas sodium benzoate (C_6H_5COONa) and sodium terephthalate (p-$C_6H_4(COONa)_2$) are chosen as representative organic salts. Significantly different effects between organic and inorganic salts on the aggregation of the gemini surfactants have been observed. In particular, the different interaction approaches of C_6H_5COONa and p-$C_6H_4(COONa)_2$ with the surfactants are discussed.

Experimental Section

Materials. Cationic gemini surfactants 12-4-12 and 12-4(OH)$_2$-12 were synthesized and purified according to the method of Zana et al.[36] Sodium chloride (≥99.5%), sodium hydroxide (≥96%), and anhydrous sodium sulfate (≥97.0%) were purchased from Beijing Chemical Reagent Company. Sodium benzoate was purchased from Sinopharm Chemical Reagent. Terephthalate acid (≥99%) was purchased from Shanghai Shiyi Chemical Reagent. Terephthalate acid was suspended in water, neutralized by the addition of a double-molar volume of sodium hydroxide, and then recrystallized and freeze-dried prior to use. Triply distilled water was used in all experiments. Both sodium benzoate (pK_a = 3.54) and sodium terephthalate (pK_1 = 3.54 and pK_2 = 4.46) were ionized in the aqueous solutions.

Turbidimetric Titration. The turbidity of 12-4-12 and 12-4(OH)$_2$-12 at different salt concentrations, reported as 100 − %T, was measured at 450 nm using a Brinkmann PC920 probe colorimeter equipped with a thermostatted water-circulating bath. The temperature was kept at 30.0 ± 0.1 °C. The final turbidity titration curves were recorded only after the values became stable (∼2−4 min). Triply distilled water was used as the standard sample, the turbidity of which was set to zero.

Surface Tension Measurement. Surface tension measurements were carried out by drop volume method[37] at 30.00 ± 0.05 °C.

Isothermal Titration Microcalorimetry (ITC). Calorimetric measurements were conducted using a TAM 2277-201 microcalorimetric system (Thermometric AB, Järfälla, Sweden) with a stainless steel sample cell of 1 mL at 30.00 ± 0.01 °C. The cell was initially loaded with 0.8 mL of 5 mM 12-4-12 or 12-4(OH)$_2$-12 solution. The concentrated salt solution was injected in the sample cell via a 500 μL Hamilton syringe controlled by a 612 Thermometric Lund pump. A series of injections was made until the desired range of concentration had been covered. The system was stirred at 50 rpm with a gold propeller. The observed enthalpy (ΔH_{obsd}) was obtained by integration over the peak for each injection in the plot of heat flow P against time t.

TABLE 1: Critical Concentrations (millimoles) of Salts at Which Salting-Out Phenomenon Happens in 10 mM Surfactant Aqueous Solutions

	NaCl	Na_2SO_4	C_6H_5COONa	p-$C_6H_4(COONa)_2$
12-4-12	520 ± 10	NA[a]	100 ± 10	850 ± 100
12-4(OH)$_2$-12	410 ± 10	15 ± 5	22 ± 2	10 ± 2

[a] No salting-out phenomenon.

^{1}H NMR Measurements. ^{1}H NMR spectra were recorded using a Bruker AV400 FT-NMR spectrometer operating at 400.1 MHz at room temperature of 23 ± 2 °C. Deuterium oxide (99.9%) was purchased from CIL (Cambridge Isotope Laboratories) and used to prepare the stock solutions of the cationic gemini surfactants with or without salts. About 1 mL of solution was transferred to a 5 mm NMR tube for each measurement. Chemical shifts were given on the δ scale. The center of the HDO signal (4.790 ppm) was used as the reference in the D_2O solutions. The digital resolution of NMR spectra was 0.04 Hz/data point. The signal assignments of the surfactants were determined by 2D NMR method (^{1}H−^{1}H COSY).

Dynamic Light Scattering (DLS). Measurements were carried out at 30.0 ± 0.5 °C by an LLS spectrometer (ALV/SP-125) with a multi-τ digital time correlator (ALV-5000). A solid-state He−Ne laser (output power of 22 mW at λ = 632.8 nm) was used as a light source, and the measurements were conducted at a scattering angle of 90°. The freshly prepared samples were injected into a 7 mL glass bottle through a 0.45 μm filter prior to measurements. The correlation function of scattering data was analyzed via the CONTIN method to obtain the distribution of diffusion coefficients (D) of the solutes; then, the apparent equivalent hydrodynamic radius (R_h) was determined using the Stokes−Einstein equation $R_h = kT/6\pi\eta D$, where k is the Boltzmann constant, T, is the absolute temperature, and η is the solvent viscosity.

Transmission Electron Microscopy (TEM). The samples were imaged under a JEM-200CX electron microscope at a working voltage of 100 kV. And the TEM samples were prepared by negative-staining method[38] and freeze-fracture technique.[39,40] As for the negative-staining method, a carbon Formvar-coated copper grid (300-mesh) was laid on one drop of the sample solution and then was put onto one drop of uranyl acetate solution (1%); finally, the excess liquid was wiped with filter paper. For the freeze-fracture technique, fracturing and replication were carried out in a high-vacuum freeze-etching system (Balzers BAF-400D).

Results and Discussion

Salting-Out Phenomenon. As the salt concentration increases, a sudden increase in turbidity is a sign of a macroscopic phase separation in a surfactant solution,[9] which is the salting-out phenomenon. The related turbidity curves for 10 mM 12-4-12 and 12-4(OH)$_2$-12 solutions with NaCl, Na_2SO_4, C_6H_5COONa, and p-$C_6H_4(COONa)_2$ are shown in the Supporting Information (Figure SI1). The critical concentrations of the salts for the salting-out of these two surfactants (Table 1) are determined from the concentration ranges of the sharply increasing turbidity in the turbidity curves. For C_6H_5COONa and p-$C_6H_4(COONa)_2$, the values for 12-4-12 solution are about one order of magnitude larger than those for 12-4(OH)$_2$-12 solution. In particular, with the addition of Na_2SO_4, even no

salting-out phenomenon happens in 12-4-12 solution within the limitation of the Na_2SO_4 solubility, whereas only ~15 mM Na_2SO_4 makes 12-4(OH)$_2$-12 salt out. That is to say, the salting-out phenomenon is very complex, which depends on not only the nature of salts but also the spacers of the gemini surfactants. Interestingly, the critical concentrations of the salts for the salting-out of 12-4(OH)$_2$-12 are much lower than those for 12-4-12. This indicates that 12-4(OH)$_2$-12 with two hydroxyl groups in the spacer prefers to salt out. According to hydration theory,[4] the two hydroxyls may form intermolecular hydrogen bonds that further break hydrated water molecules around the 12-4(OH)$_2$-12 molecules and cause the surfactant molecules to salt out more easily.

Salt Effects on CMC and Surface Activity. The surface tension curves of 12-4-12 and 12-4(OH)$_2$-12 in aqueous solutions without salts are shown in Figure SI2 of the Supporting Information, and the surface tension curves of 12-4-12 and 12-4(OH)$_2$-12 at different concentrations of NaCl, Na_2SO_4, C_6H_5COONa, and p-$C_6H_4(COONa)_2$ are presented in Figures 2 and 3. The CMC values determined from the surface tension curves are plotted against the ionic strengths of added salts in Figure 4.

For the pure surfactants in aqueous solutions without any added salts, the CMC value of 12-4(OH)$_2$-12 (0.7 mM) is lower than that of 12-4-12 (1.1 mM). The CMC values are in good agreement with literature values.[24] As discussed above, the two hydroxyls may form intermolecular hydrogen bonds among the 12-4(OH)$_2$-12 molecules, which may effectively promote the aggregation of 12-4(OH)$_2$-12 molecules.

In the presence of the four inorganic and organic salts, with the increase in the ionic strength, the CMC values of these two surfactants decrease sharply at first and then decrease much more slowly or almost level off (Figure 4). The increased ionic strength can effectively reduce the electrostatic repulsion between the intermolecular headgroups. The electrostatic repulsion may become almost invariable once the ionic strength is large enough; then, the CMC values become constant.[41] The ability of reducing CMC is in the order of C_6H_5COONa > p-$C_6H_4(COONa)_2$ > Na_2SO_4> NaCl at the same ionic strength. Organic salts are more efficient to promote the aggregation of the gemini surfactants than inorganic salts.

As for surface activity, the surface tension values at CMC (γ_{cmc}) are plotted against the salt concentration in Figure SI3 of the Supporting Information. The experimental error of the surface tension is ±1 mN/m. As shown, NaCl, $NaSO_4$, and p-$C_6H_4(COONa)_2$ almost do not affect the γ_{cmc} values considering the experimental errors. However, C_6H_5COONa greatly decreases the γ_{cmc} values. That is to say, only C_6H_5COONa can distinctly reduce both CMC and γ_{cmc} values, indicating that $C_6H_5COO^-$ anions can greatly enhance the close packing of the cationic gemini surfactant molecules at air−water interface.

Salt Effects on Morphology of the Surfactant Aggregates. To understand the structure variation of the surfactant aggregates, we have studied the salt effects on the aggregate size and morphology of the gemini surfactants beyond the CMC values. The size distributions of the aggregates of 5 mM 12-4-12 and 12-4(OH)$_2$-12 at different salt concentrations from DLS measurements are shown in Figure 5. The obtained hydrodynamic radii (R_h) of the surfactant aggregates at different salt concentrations are summarized in the Supporting Information (Figure SI4).

For 12-4(OH)$_2$-12 (Figure 5b,d,f,h), two size distributions at 1−3 nm and ~70 nm are observed at low salt concentrations or without any salts. The large aggregates are vesicles approved

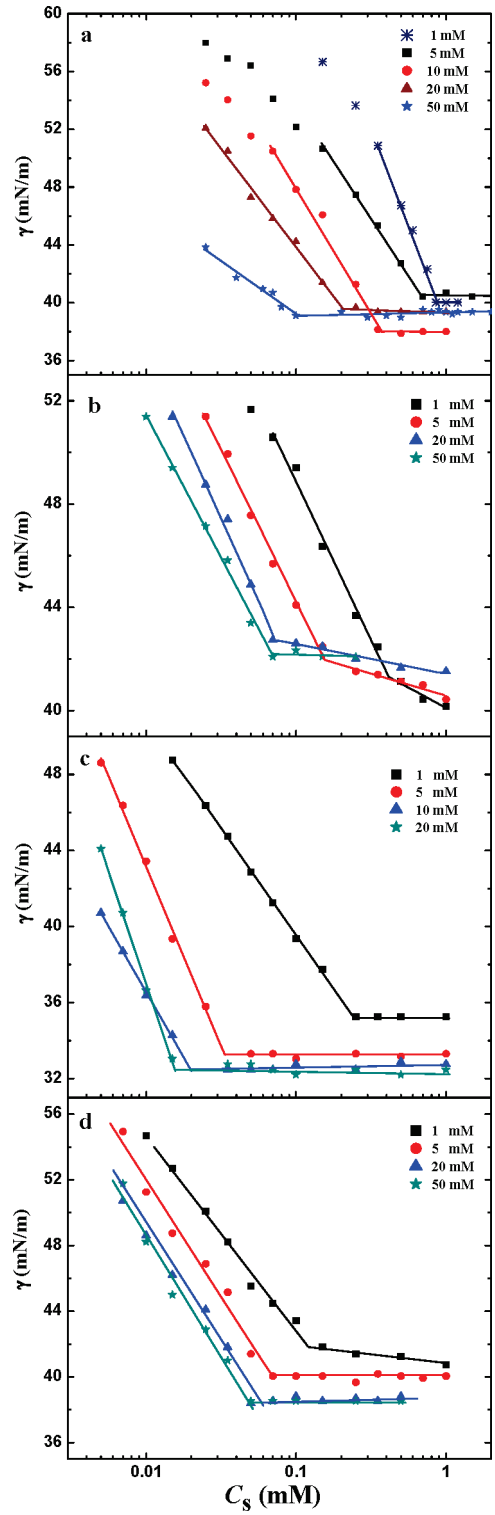

Figure 2. Surface tension curves of 12-4-12 plotted against the surfactant concentration (C_s) at different salt concentrations: (a) NaCl, (b) Na_2SO_4, (c) C_6H_5COONa, and (d) p-$C_6H_4(COONa)_2$.

by TEM images (Figure SI5 of Supporting Information). The small size distribution at 1−3 nm should correspond to micelles but is smaller than the real size of the micelles because the high charge density of the gemini surfactant micelles affects the DLS measurement. From the DLS theory, scattered intensity is roughly proportional to the sixth power of particle size. From the relative intensity, it is concluded that the number of vesicles is smaller than that of the micelles in the 12-4(OH)$_2$-12 solutions. As the salt concentrations increase, the vesicle peak gradually

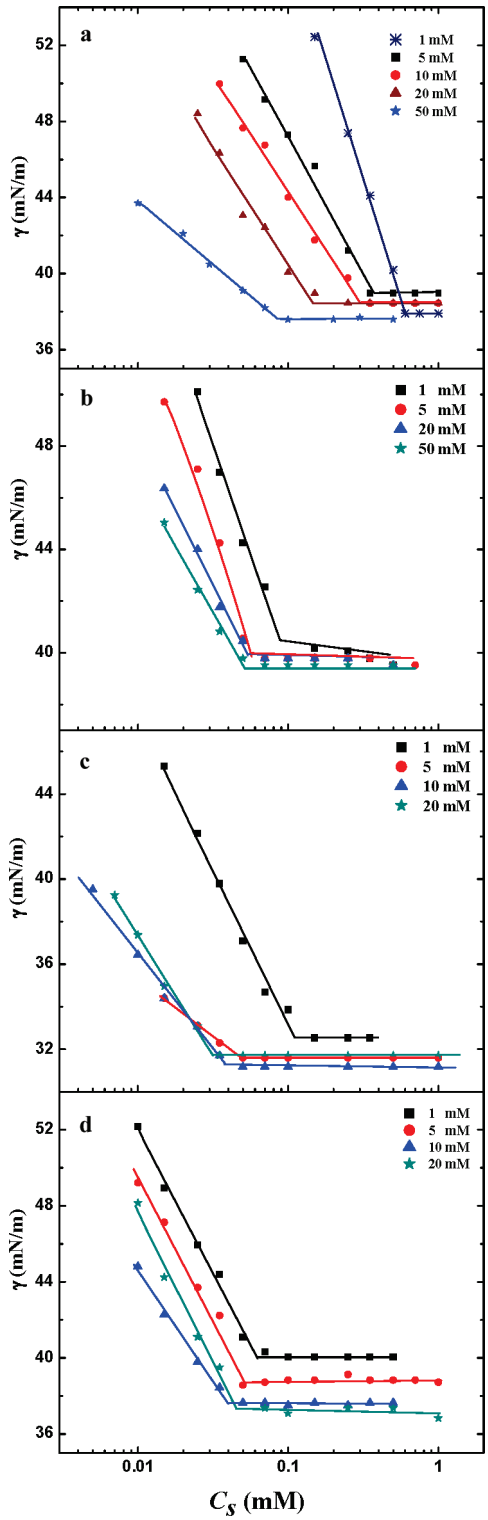

Figure 3. Surface tension curves of 12-4(OH)$_2$-12 plotted against the surfactant concentration (C_s) at different salt concentrations: (a) NaCl, (b) Na_2SO_4, (c) C_6H_5COONa, and (d) p-$C_6H_4(COONa)_2$.

becomes smaller and disappears at last. The salts can disrupt the structures of the vesicles possibly through compressing the double layer of vesicles.[42,43] It is noted that the hydrodynamic radii (R_h) of the micelles only slightly increase with the addition of NaCl, Na_2SO_4, and p-$C_6H_4(COONa)_2$, whereas the increase in C_6H_5COONa concentration leads to a more significant growth of the 12-4(OH)$_2$-12 micelles. These results indicate that the 12-4(OH)$_2$-12 system changes from the micelle/vesicle coexistence to vesicles with the addition of C_6H_5COONa (Figure 6b),

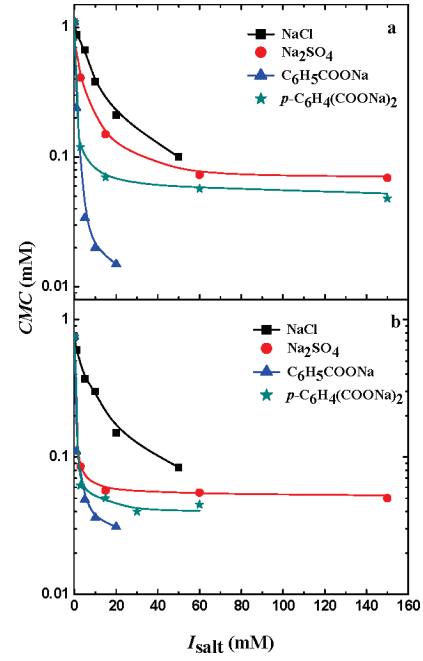

Figure 4. Plots of logarithm of the CMC values of (a) 12-4-12 and (b) 12-4(OH)$_2$-12 against the ionic strength (I_{salt}) of added salts.

whereas the other three salts transfer the 12-4(OH)$_2$-12 system from the micelle/vesicle coexistence to micelles. The formation of vesicles in cationic gemini surfactant solutions with the addition of organic salts was also previously observed.[29,32]

However, all DLS results display only one peak for the 12-4-12 aqueous solutions at different salt concentrations (Figure 5a,c,e,g). The hydrodynamic radius of the 12-4-12 micelles only slightly increases with the increase in the NaCl, Na_2SO_4, and p-$C_6H_4(COONa)_2$ concentration, whereas the aggregate size of 12-4-12 increases more significantly with the addition of C_6H_5COONa. The vesicles upon the addition of C_6H_5COONa were observed by the FF-TEM method shown in Figure 6a.

Enthalpy Change upon Interaction of Salts with Surfactant Aggregates. Microcalorimetry is an effective tool to monitor the enthalpy change during the molecular interaction process. Here we have studied the processes of the concentrated salts being titrated in the 5 mM surfactant solutions and in water by ITC. The observed enthalpy changes (ΔH_{obsd}) with the final salt concentration (C_{salt}) are plotted in Figure 7. During the titrations, the concentrations of the surfactant solutions hardly change because the changes of the total solution volume in the sample cell are within 0.15 mL, which can be neglected. For all four salts, the measured dilution enthalpy changes in water are close to zero. Therefore, all titration curves of the salts in the surfactant solutions can be thought of as the interaction of the salts with the surfactants.

It is noted that the changing situations for 12-4-12 and 12-4(OH)$_2$-12 are the same for the same salt. With the addition of NaCl to the 12-4-12 and 12-4(OH)$_2$-12 solutions, the ΔH_{obsd} values are close to zero, slightly increasing from very small negative values to very small positive values. However, the additions of Na_2SO_4, p-$C_6H_4(COONa)_2$, and C_6H_5COONa induce significant enthalpy changes. For both Na_2SO_4 and p-$C_6H_4(COONa)_2$, the variations of the enthalpy are very similar; that is, an obvious endothermic peak emerges. Because electrostatic binding between the oppositely charged surfactants and Na_2SO_4 or p-$C_6H_4(COONa)_2$ should result in exothermic enthalpy changes, the observed endothermic changes may be caused by the strong dehydration of dianions accompanied by

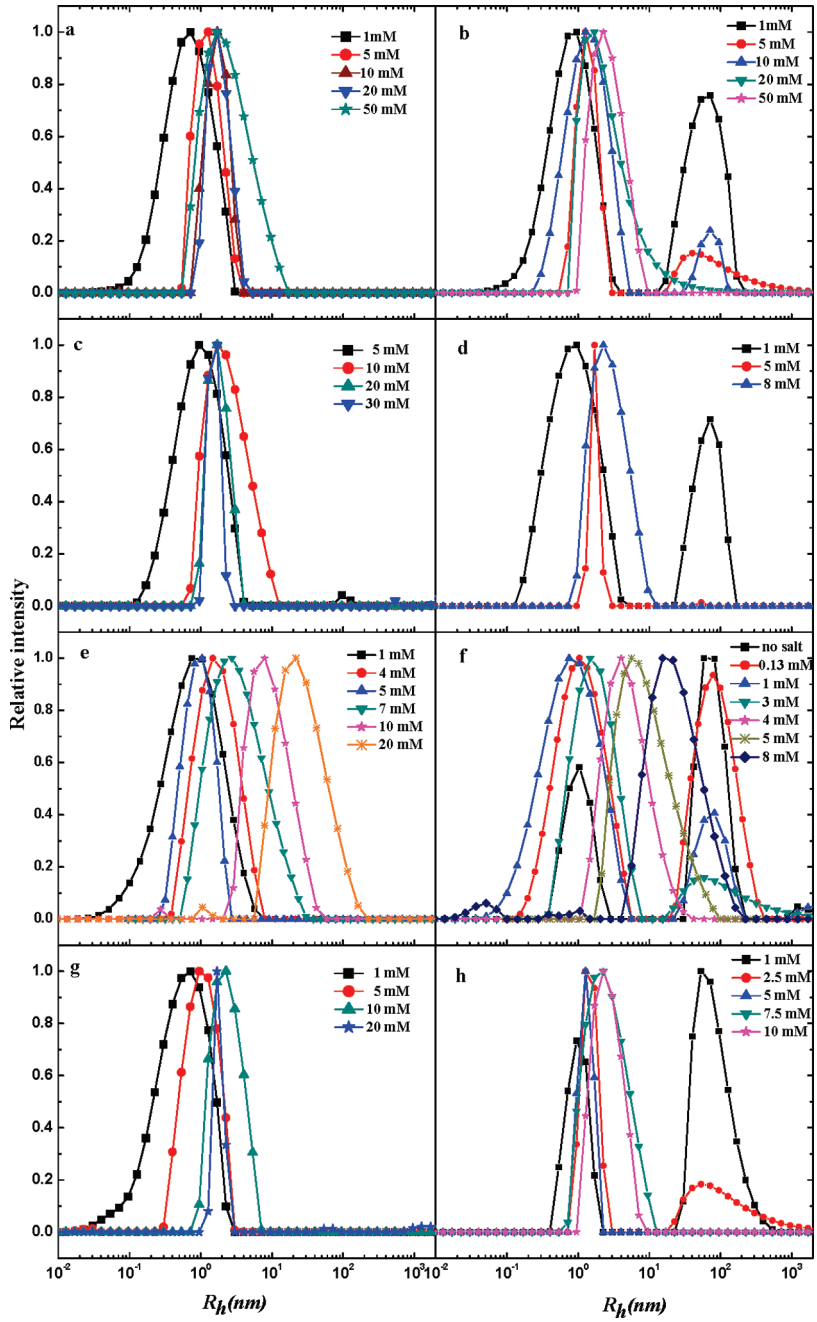

Figure 5. Size distributions of 5 mM gemini surfactants at different salt concentrations (indicated in the plots) at 30.0 °C. (a) NaCl + 12-4-12; (b) NaCl + 12-4(OH)$_2$-12; (c) Na_2SO_4 + 12-4-12; (d) Na_2SO_4 + 12-4(OH)$_2$-12; (e) C_6H_5COONa + 12-4-12; (f) C_6H_5COONa + 12-4(OH)$_2$-12; (g) *p*-$C_6H_4(COONa)_2$ + 12-4-12; and (h) *p*-$C_6H_4(COONa)_2$ + 12-4(OH)$_2$-12.

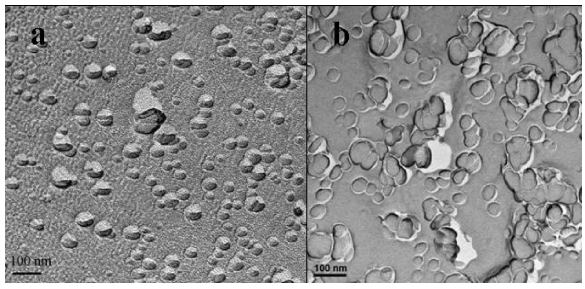

Figure 6. FF-TEM micrograph: (a) 5 mM 12-4-12 solution with 20 mM C_6H_5COONa and (b) 5 mM 12-4(OH)$_2$-12 solution with 8 mM C_6H_5COONa.

the electrostatic binding. When the dianions are saturated in the palisade layer of the aggregates, the dehydration effect disappears, and hence the positive ΔH_{obsd} values almost level off and change to zero. The saturated adsorption concentration (SAC) at the surface of surfactant aggregates is estimated from the intersection of the two tangent lines, as shown in Figure 7. The SACs of SO_4^{2-} and *p*-$C_6H_4(COO^-)_2$ are ~5 mM for both 5 mM 12-4-12 and 12-4(OH)$_2$-12 solutions. As for C_6H_5COONa, the variation of ΔH_{obsd} is totally different from the cases of Na_2SO_4 and *p*-$C_6H_4(COONa)_2$. The ΔH_{obsd} value is large exothermic value at low C_6H_5COONa concentration and decreases with the increase in the C_6H_5COONa concentration. Then, an obvious exothermic peak presents in the calorimetric titration curves; finally, the curves become close to zero. The different calorimetric curves indicate that C_6H_5COONa interacts with the surfactants in a different way from the other three salts. The large exothermic enthalpy changes at low C_6H_5COONa

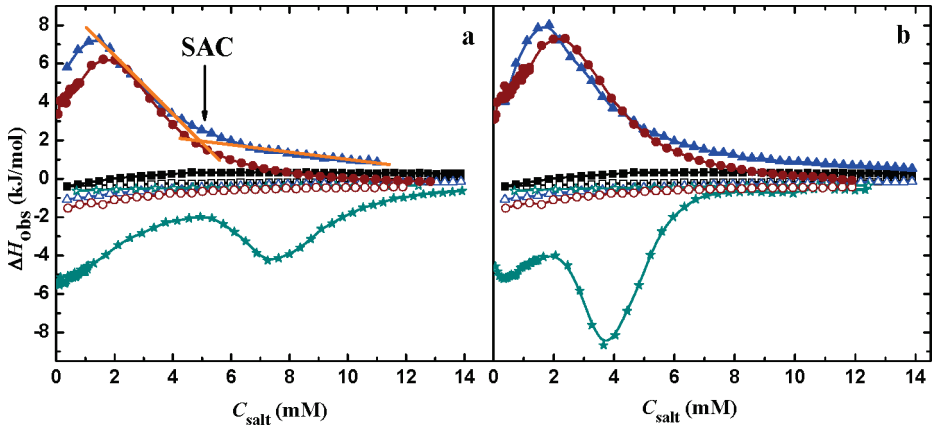

Figure 7. Observed enthalpy ΔH_{obsd} versus the total salt concentration C_{salt} for the titration of concentrated salt solutions in (a) 5 mM 12-4-12 and (b) 12-4(OH)$_2$-12 solutions or triply distilled water at 30.0 °C. (□) NaCl + H_2O; (■) NaCl + surfactant; (△) Na_2SO_4 + H_2O; (▲) Na_2SO_4 + surfactant; (☆) C_6H_5COONa + H_2O; (★) C_6H_5COONa + surfactant; (○) p-$C_6H_4(COONa)_2$ + H_2O; (●) p-$C_6H_4(COONa)_2$ + surfactant. Determination of the saturated adsorption concentration (SAC) of Na_2SO_4 at the surface of 12-4-12 aggregates from the calorimetric curve of Na_2SO_4 solution.

concentration should be caused by the electrostatic binding of $C_6H_5COO^-$ anions with the cationic headgroups of the surfactants. The following exothermic peak may be directly related to the morphology changes from micelles to vesicles in 12-4-12 and 12-4(OH)$_2$-12 solutions induced by C_6H_5COONa, which will be discussed in the latter text.

Variation of Proton Microenvironment upon Interaction between Surfactants and Salts. To reveal the intermolecular interaction in the salt-surfactant systems, ^{1}H NMR technique is applied. ^{1}H NMR spectra of the pure 12-4-12 and 12-4(OH)$_2$-12 in D_2O are shown in Figure SI6 and their ^{1}H−^{1}H COSY spectra are shown in Figures SI7 and SI8 of the Supporting Information. The hydrogen atoms on various carbons are labeled as shown in Figure 1. The surfactant concentration used is 2 mM, which is about twice as large as their CMC. Therefore, the observed chemical shifts basically reflect the protons of the surfactant molecules in the aggregates. The protons of the hydroxyl groups of 12-4(OH)$_2$-12 have no signals because they are exchanged fast by deuterium. Figures 8 and 9 show the chemical shifts in the ^{1}H NMR spectra of 12-4-12 and 12-4(OH)$_2$-12 solutions at different concentrations of NaCl, Na_2SO_4, C_6H_5COONa, and p-$C_6H_4(COONa)_2$. The variations of the chemical shifts for the present surfactant systems are different for different salts.

Inorganic salts NaCl and Na_2SO_4 do not generate significant variations of the chemical shifts of the protons for both 12-4-12 and 12-4(OH)$_2$-12, confirming that the surfactant aggregates do not have any remarkable changes upon the addition of NaCl and Na_2SO_4. With the addition of NaCl, the chemical shifts of all the protons of 12-4-12 and 12-4(OH)$_2$-12 only slightly move downfield and then become almost invariable when the NaCl concentration reaches 10 mM. It indicates that the adsorption of Cl^- at the double layer of the surfactant aggregates has been saturated with 10 mM concentration and more Cl^- would stay in the bulk solutions in the form of free ions. Because the Cl^- ions reduce the electrostatic repulsion among the surfactant headgroups and promote the surfactant aggregation, the protons move downfield. However, with the addition of Na_2SO_4, the chemical shifts slightly shift to downfield for the protons (a-H and b-H) in the interior of micellar cores for both 12-4-12 and 12-4(OH)$_2$-12, whereas they shift to upfield for those near the ammonium headgroups, except the protons (f-H) on the methyl groups connected to the ammonium headgroups of 12-4-12. SO_4^{2-} exhibits stronger binding ability with the ammonium headgroups of cationic gemini surfactant because it owns much

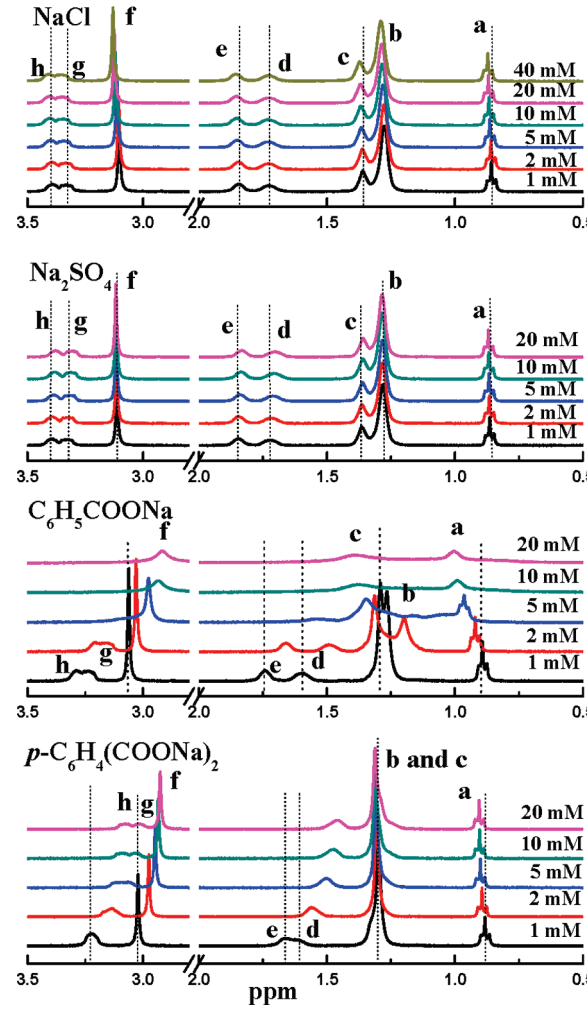

Figure 8. ^{1}H NMR spectra of 2 mM 12-4-12 with various concentrations of salts.

higher electrovalence and larger electronegativity than Cl^-.[44] This promotes the surfactant aggregation and also gets the protons around the headgroups shielded. Therefore, the chemical shifts for almost all protons around the headgroups move upfield.

Differently, organic salts C_6H_5COONa and p-$C_6H_4(COONa)_2$ cause significant changes of the chemical shifts of the protons for both 12-4-12 and 12-4(OH)$_2$-12. With the addition of C_6H_5COONa, the chemical shifts of the protons in the alkyl

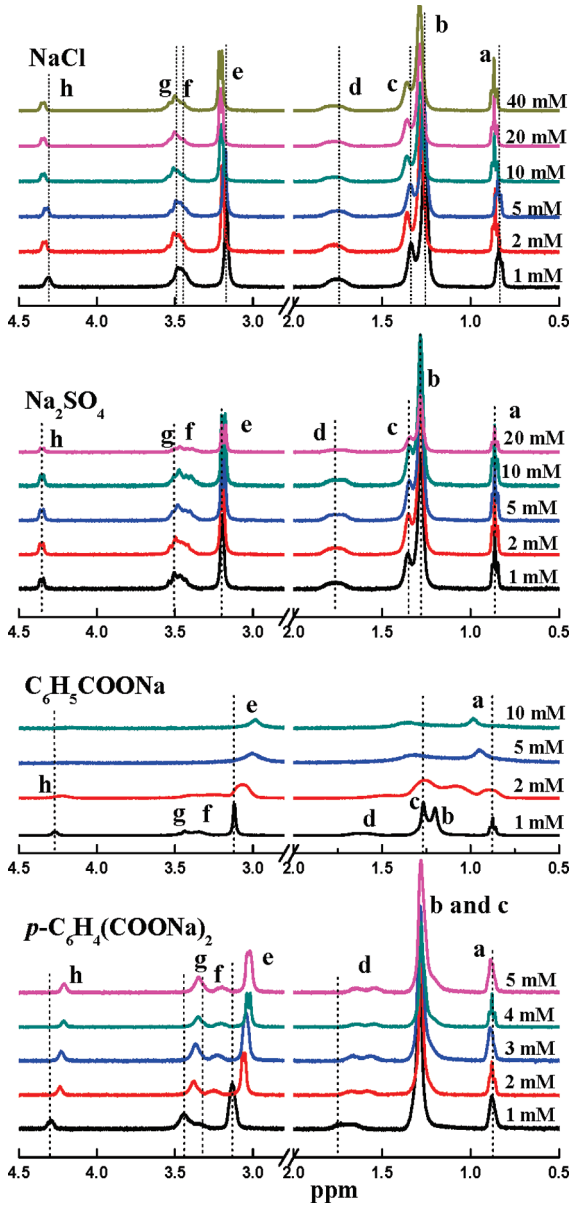

Figure 9. ^{1}H NMR spectra of 2 mM 12-4(OH)$_2$-12 with various concentrations of salts.

chains (a-H, b-H, and c-H) move downfield, and the movements are much more significant than those with the other salts. Meanwhile, the peak of the b-H proton gradually merges into that of the c-H proton, whereas the protons near the ammonium headgroups move upfield significantly. In particular, the peaks of d-H, e-H, g-H, and h-H protons for 12-4-12 and the peaks of d-H, f-H, g-H and h-H protons for 12-4(OH)$_2$-12 disappear when the C_6H_5COONa concentration reaches 5 mM, and all of the peaks gradually become broadened. The interaction of aromatic anions with ammonium groups may reduce the tendency to withdraw electrons from the carbon atoms attached to the headgroups, leading to the upfield shift of the protons near the ammonium headgroup. The phenyl group of C_6H_5COONa may penetrate into the hydrophobic cores of the surfactant aggregates, which makes the protons in the alkyl chains be shielded and the chemical shifts move upfield. However, the micelle-to-vesicle transition with the addition of C_6H_5COONa causes the chemical shifts of the protons in the alkyl chains to move downfield greatly. The probable reason of the peak broadening and disappearance is that the motion of the surfactant molecules is highly restricted in vesicle phase.[45−47] As for the addition of p-$C_6H_4(COONa)_2$, for both 12-4-12 and 12-4(OH)$_2$-12, the chemical shifts slightly shift to downfield for the protons (a-H and b-H) of the hydrophobic side chains, and the c-H peak shifts upfield and merges into the b-H peak, but the protons around the headgroups shift to upfield. Obviously, the benzene ring of C_6H_5COONa contacts more closely with the hydrophobic core of the surfactant aggregates than that of p-$C_6H_4(COONa)_2$.

The variation of the ^{1}H NMR spectra of these two organic salts in the surfactant solutions can also reflect their interaction approach with the surfactants. The chemical shifts of the protons of C_6H_5COONa and $C_6H_4(COONa)_2$ in 5 or 2 mM surfactant solutions are shown in Figures 10 and 11 and Figure SI9 of the Supporting Information. As the concentration of C_6H_5COONa and p-$C_6H_4(COONa)_2$ increases, the chemical shifts of their protons move upfield at first, then gradually get close to those of pure C_6H_5COONa and p-$C_6H_4(COONa)_2$ without any surfactants because excess salts become a main component. For p-$C_6H_4(COONa)_2$, all protons (2-H, 3-H, 5-H, and 6-H) only shift downfield slightly, suggesting that p-$C_6H_4(COO^-)_2$ anions still stay in a polar environment. It can be imagined that the strong electrostatic interaction between the two carboxyl groups of $C_6H_4(COONa)_2$ and the charged headgroups of the surfactants prevents the benzene ring of p-$C_6H_4(COO^-)_2$ to penetrate into the surfactant aggregates. However, as for C_6H_5COONa, the 3-H, 4-H, and 5-H protons are shifted upfield by the surfactants, whereas 2-H and 6-H protons are moved downfield. In general, aromatic protons shift upfield in less polar environment because of the decrease in the deshielding effect. This means the 3-H, 4-H, and 5-H protons of C_6H_5COONa exist in a relatively nonpolar environment, whereas the 2-H and 6-H protons exist in a polar environment. The average chemical shifts of the 3-H and 5-H protons of C_6H_5COONa are plotted against the C_6H_5COONa concentration in Figure 12. The 3-H and 5-H protons of C_6H_5COONa cannot be distinguished in the spectra, and thus the average chemical shifts are used. As the concentration of C_6H_5COONa increases, the 3-H and 5-H protons move upfield at first and then gradually shift downfield, which means that $C_6H_5COO^-$ anions may penetrate into the hydrophobic core and excess $C_6H_5COO^-$ anions will stay in the bulk solution as free ions. The turning point should be the saturated C_6H_5COONa concentration of penetrating into the hydrophobic cores of the surfactant aggregates, which are about 8.9 and 4.9 mM in the 12-4-12 and 12-4(OH)$_2$-12 solutions, respectively. Obviously, the saturated concentration for 12-4(OH)$_2$-12 solution is much lower than that for 12-4-12 solution. The probable reason is that the steric effect of the hydroxyls would allow fewer $C_6H_5COO^-$ anions to insert into the hydrophobic cores of the surfactant aggregates.

Mechanism of Salt Effect on Surfactant Aggregation. The above results reveal that the valence and structure of salts play an important role in the aggregation behavior of cationic gemini surfactants. Inorganic salts affect surfactant aggregation mainly through reducing the electrostatic interaction among the surfactant headgroups, and SO_4^{2-} is more efficient to promote the aggregation of the gemini surfactants than Cl^- .

Interestingly, the organic salts affect the aggregation of the surfactants in different ways. The proposed schematic illustrations of $C_6H_5COO^-$ and p-$C_6H_4(COO^-)_2$ anions at the air−water and water−aggregate interface are shown in Scheme 1. For p-$C_6H_4(COONa)_2$, the two carboxyl groups are located at the para positions of benzene ring. Both the hydrophobic interaction of benzene ring with the surfactant molecules and the electro-

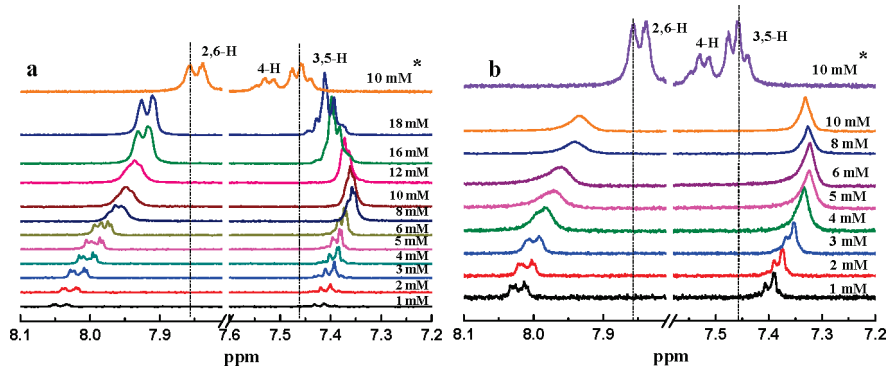

Figure 10. ^{1}H NMR spectra of C_6H_5COONa of different concentrations with 5 mM (a) 12-4-12 and (b) 12-4(OH)$_2$-12. *10 mM C_6H_5COONa without surfactants.

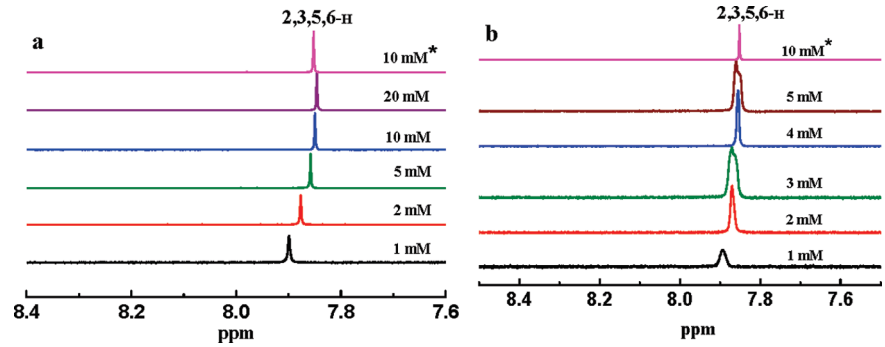

Figure 11. ^{1}H NMR spectra of p-$C_6H_4(COONa)_2$ of different concentrations with 2 mM (a) 12-4-12 and (b) 12-4(OH)$_2$-12. *10 mM p-$C_6H_4(COONa)_2$ without surfactants.

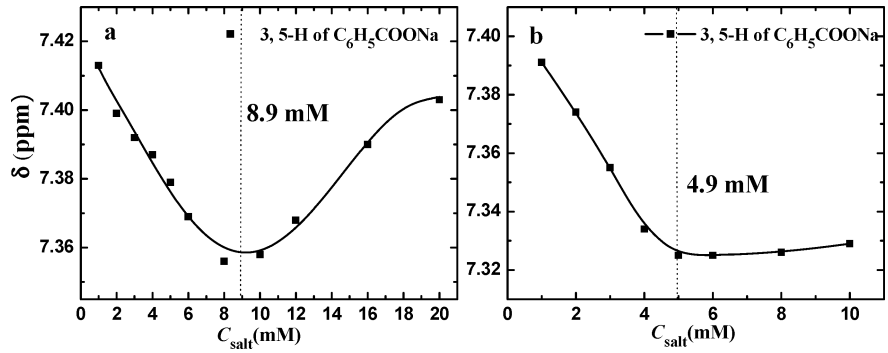

Figure 12. Chemical shifts of 3,5-H of C_6H_5COONa against the C_6H_5COONa concentration with 5 mM (a) 12-4-12 and (b) 12-4(OH)$_2$-12.

static binding of negatively charged COO^- with the cationic charged headgroups of the surfactants cannot be effectively realized at the same time. Therefore, p-$C_6H_4(COO^-)_2$ anions cannot penetrate into the hydrophobic cores. According to the CPK models, the distance between the two carboxyl groups of p-$C_6H_4(COO^-)_2$ anion is estimated to be 0.58 nm and matches the dimensions between the two gemini charges, which is ~0.62 nm. Therefore, p-$C_6H_4(COO^-)_2$ anion affects the surfactant aggregation only through reducing the electrostatic repulsion, like the inorganic salts, as shown.

Of particular interest is that C_6H_5COONa reduces the CMC of the surfactants much more significantly than p-$C_6H_4(COONa)_2$ and induces the micelle-to-vesicle transition. Its carboxyl group favors the water phase, whereas its benzene ring favors the hydrophobic phase. Both factors can be satisfied when $C_6H_5COO^-$ anions insert into the surfactant micelles with the benzene ring located in the hydrophobic microdomain. So C_6H_5COONa greatly lowers the electrostatic repulsion between the headgroups of the gemini surfactants and makes the hydrophobic chains arrange more closely, which causes the micelle-to-vesicle transition. In addition, the charge neutralization is an important factor to promote this morphology change. Combined with the variations of enthalpy, the aggregate size, and the surface tension with the C_6H_5COONa concentration, the critical transition concentrations of C_6H_5COONa required for the surfactants to transfer from micelles to vesicles (CTC) are shown in Figure 13, which are 7.5 ± 0.3 and 3.7 ± 0.4 mM in 5 mM 12-4-12 and 12-4(OH)$_2$-12 solution, respectively. When the C_6H_5COONa concentration exceeds the CTC, the average hydrodynamic radius (R_h) of the surfactant aggregates starts to increase sharply because of the occurrence of the micelle-to-vesicle transition. Meanwhile, the surface tension decreases first and then becomes constant beyond the CTC, which also reflects the formation of different assemblies.[48,49] Besides, the aggregate transition caused by C_6H_5COONa is also reflected in the obvious peak broadening and peak disappearance of some protons of the surfactants in ^{1}H NMR spectra beyond the CTC (Figures SI10 and SI11 of the Supporting Information).

Another interesting point is that the surfactant spacers also influence the salt effect on the aggregation behavior of the

SCHEME 1: Proposed Schematic Illustrations of C_6H_5COONa (Upper) at Air−Water Interface and Water−Vesicle Interface and *p*-$C_6H_4(COONa)_2$ (Lower) at Air−Water Interface and Water−Micelle Interface[a]

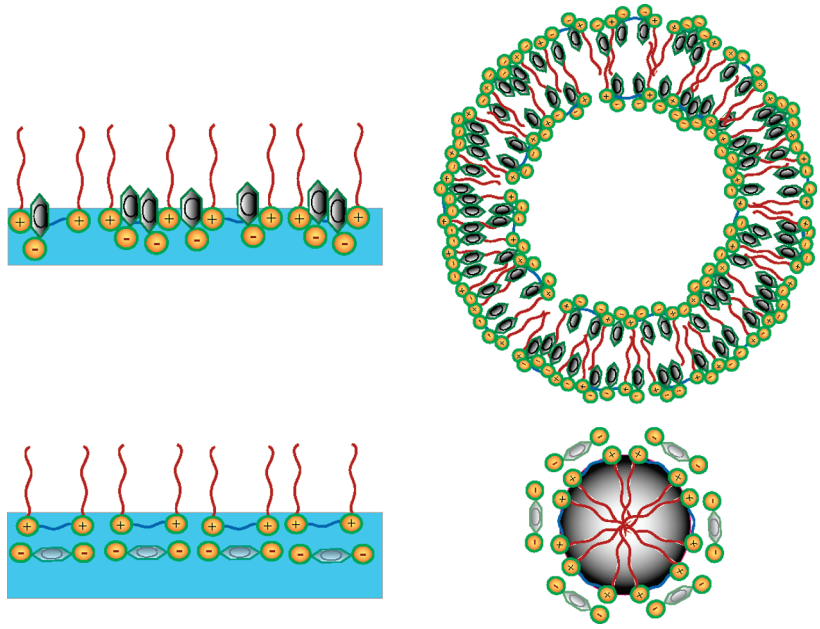

[a] 12-4-12 and 12-4(OH)$_2$-12 are modeled with two spherical heads, two flexible tails and a spacer chain. Br^- and Na^+ are not shown.

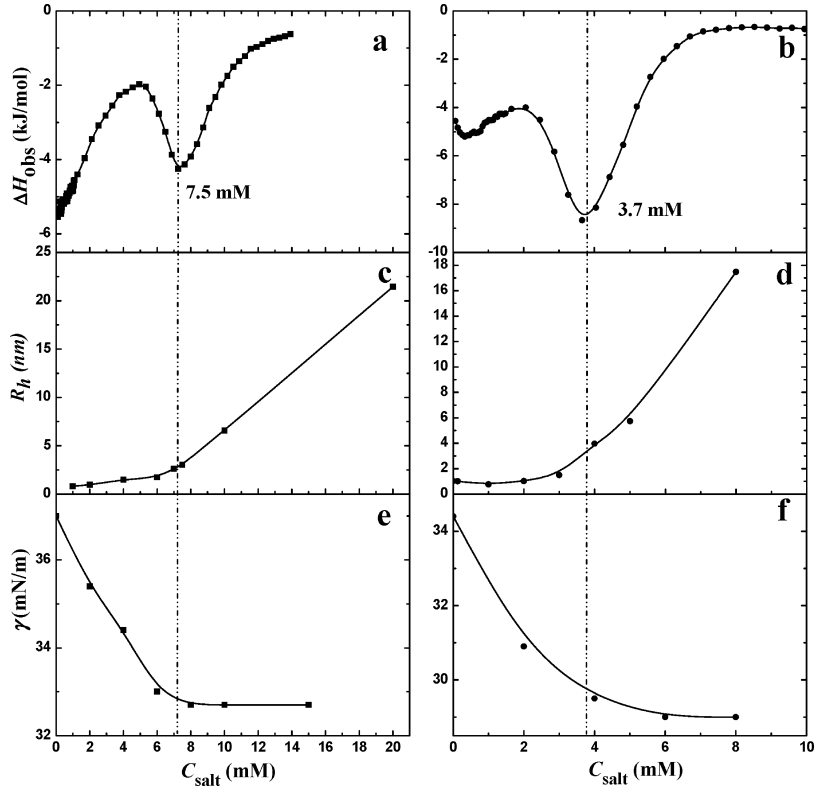

Figure 13. Observed enthalpy, ΔH_{obsd}, hydrodynamic radius (R_h), and surface tension of 5 mM (a,c,e) 12-4-12 and (b,d,f) 12-4(OH)$_2$-12 as a function of C_6H_5COONa concentration.

gemini surfactants. The additional hydroxyls in 12-4(OH)$_2$-12 may form intermolecular hydrogen bonds, effectively enhancing the aggregation ability. Therefore, the 12-4(OH)$_2$-12 solution needs a much smaller amount of $C_6H_5COO^-$ anions to induce the morphology changes.

Conclusions

The effects of inorganic and organic salts on the aggregation behavior of the gemini surfactants 12-4-12 and 12-4(OH)$_2$-12 with a hydrophobic or hydrophilic spacer have been studied. Both inorganic and organic salts effectively reduce the CMC values of these two surfactants. The ability to promote the surfactant aggregation decreases in the order of C_6H_5COONa > *p*-$C_6H_4(COONa)_2$ > Na_2SO_4 > NaCl. Because the benzene rings of organic salts are somewhat hydrophobic, organic salts are more effective to promote the aggregation. In particular, only C_6H_5COONa can reduce both the CMC values and the γ_{cmc} values because of the hydrophobic interaction between

$C_6H_5COO^-$ anions and the hydrophobic chains at the air−water interface. Without any salts, vesicles and micelles coexist in 12-4(OH)$_2$-12 solution, whereas only micelles exist in 12-4-12 solution. As for the 12-4-12 solution, the penetration of $C_6H_5COO^-$ anions and the charge neutralization of the surfactant by $C_6H_5COO^-$ induce a micelle-to-vesicle change, whereas the other three salts only slightly increase the micelle sizes. However, the 12-4(OH)$_2$-12 solution changes from the micelle/vesicle coexistence of to vesicles with the addition of C_6H_5COONa, whereas the other salts transfer the 12-4(OH)$_2$-12 solution from the micelle/vesicle coexistence to micelles. Similar to the inorganic salts, *p*-$C_6H_4(COONa)_2$ only promotes the growth of the surfactant aggregates through reducing the electrostatic repulsion among the surfactant headgroups because *p*-$C_6H_4(COONa)_2$ stays at the surface of the surfactant aggregates rather than penetrating into the hydrophobic core. This work is helpful to understand the salt effects of both inorganic and organic on the aggregation behavior of gemini surfactants and suggests that applying proper organic salts can effectively adjust the structure of the surfactant aggregates.

Acknowledgment. This work was supported by the Chinese Academy of Sciences, the National Natural Science Foundation of China, and the National Basic Research Program of China (grants 20633010, 2005cb221300). We thank the State Key Laboratory of Polymer Physics and Chemistry for DLS and the Center for Biological Electron Microscopy, the Institute of Biophysics for electron microscopy work.

Supporting Information Available: Turbidity curves of 12-4-12 and 12-4(OH)$_2$-12 with different salts, surface tension curves of 12-4-12 and 12-4(OH)$_2$-12 without any additives, the γ_{cmc} values of 12-4-12 and 12-4(OH)$_2$-12 versus the salt concentration, hydrodynamic radii of 12-4-12 and 12-4(OH)$_2$-12 solutions as a function of salt concentrations, negative-staining TEM images for 5 mM 12-4(OH)$_2$-12, ^{1}H NMR and COSY spectra of 2 mM 12-4-12 and 12-4(OH)$_2$-12 in D_2O, and ^{1}H NMR spectra of 2 and 5 mM 12-4-12 with C_6H_5COONa. This information is available free of charge via the Internet at http://pubs.acs.org.

References and Notes

(1) Mukerjee, P.; Chan, C. C. *Langmuir* **2002**, *18*, 5375–5381.
(2) Long, F. A.; McDevit, W. F. *Chem. Rev.* **1952**, *51*, 119–169.
(3) Wattebled, L.; Laschewsky, A. *Langmuir* **2007**, *23*, 10044–10052.
(4) Grover, P. K.; Ryall, R. L. *Chem. Rev.* **2005**, *105*, 1–10.
(5) Corrin, M. L.; Harkins, W. D. *J. Am. Chem. Soc.* **1947**, *69*, 683–688.
(6) Aswal, V. K.; Goyal, P. S. *Chem. Phys. Lett.* **2002**, *364*, 44–50.
(7) Mu, J.-H.; Li, G.-Z.; Jia, X.-L.; Wang, H.-X.; Zhang, G.-Y. *J. Phys. Chem. B* **2002**, *106*, 11685–11693.
(8) Khatory, A.; Lequeux, F.; Kern, F.; Candau, S. J. *Langmuir* **1993**, *9*, 1456–1464.
(9) Shikata, T.; Hirata, H.; Kotaka, T. *Langmuir* **1989**, *5*, 398–405.
(10) Clausen, T. M.; Vinson, P. K.; Minter, J. R.; Davis, H. T.; Talmon, Y.; Miller, W. G. *J. Phys. Chem.* **1992**, *96*, 474–484.
(11) Hassan, P. A.; Yakhmi, J. V. *Langmuir* **2000**, *16*, 7187–7191.
(12) Bunton, C. A.; Minch, M. J.; Hidalgo, J.; Sepulveda, L. *J. Am. Chem. Soc.* **1973**, *95*, 3262–3272.
(13) Bijma, K.; Engberts, J. B. F. N. *Langmuir* **1997**, *13*, 4843–4849.
(14) Israelachvili, J. N.; John Mitchell, D.; Ninham, B. W. *J. Chem. Soc., Faraday Trans. 2* **1976**, *72*, 1525–1564.
(15) Berret, J.-F. *Molecular Gels: Materials with Self-Assembled Fibrillar Networks*; Springer: Dordrecht, The Netherlands, 2006; pp 667−720.
(16) Shikata, T.; Hirata, H.; Kotaka, T. *Langmuir* **1988**, *4*, 354–359.
(17) Rehage, H.; Hoffmann, H. *J. Phys. Chem.* **1988**, *92*, 4712–4719.
(18) Shikata, T.; Imai, S.-i.; Morishima, Y. *Langmuir* **1998**, *14*, 2020–2026.
(19) Berret, J.-F. *Langmuir* **1997**, *13*, 2227–2234.
(20) Khatory, A.; Kern, F.; Lequeux, F.; Appell, J.; Porte, G.; Morie, N.; Ott, A.; Urbach, W. *Langmuir* **1993**, *9*, 933–939.
(21) Kern, F.; Zana, R.; Candau, S. J. *Langmuir* **1991**, *7*, 1344–1351.
(22) Aswal, V. K. *J. Phys. Chem. B* **2003**, *107*, 13323–13328.
(23) Menger, F. M.; Littau, C. A. *J. Am. Chem. Soc.* **1991**, *113*, 1451–1452.
(24) Fredric, M.; Menger, J. S. K. *Angew. Chem., Int. Ed.* **2000**, *39*, 1906–1920.
(25) Zana, R. *Adv. Colloid Interface Sci.* **2002**, *97*, 203–251.
(26) Zana, R.; Talmon, Y. *Nature* **1993**, *362*, 228–230.
(27) Danino, D.; Talmon, Y.; Zana, R. *Langmuir* **1995**, *11*, 1448–1456.
(28) Ryhanen, S. J.; Saily, V. M. J.; Parry, M. J.; Luciani, P.; Mancini, G.; Alakoskela, J. M. I.; Kinnunen, P. K. J. *J. Am. Chem. Soc.* **2006**, *128*, 8659–8663.
(29) Lu, T.; Huang, J.; Li, Z.; Jia, S.; Fu, H. *J. Phys. Chem. B* **2008**, *112*, 2909–2914.
(30) Huang, X.; Cao, M.; Wang, J.; Wang, Y. *J. Phys. Chem. B* **2006**, *110*, 19479–19486.
(31) Oda, R.; Bourdieu, L.; Schmutz, M. *J. Phys. Chem. B* **1997**, *101*, 5913–5916.
(32) Buwalda, R. T.; Engberts, J. B. F. N. *Langmuir* **2001**, *17*, 1054–1059.
(33) Oda, R.; Huc, I.; Schmutz, M.; Candau, S. J.; MacKintosh, F. C. *Nature* **1999**, *399*, 566–569.
(34) Berthier, D.; Buffeteau, T.; Leger, J. M.; Oda, R.; Huc, I. *J. Am. Chem. Soc.* **2002**, *124*, 13486–13494.
(35) Brizard, A.; Aime, C.; Labrot, T.; Huc, I.; Berthier, D.; Artzner, F.; Desbat, B.; Oda, R. *J. Am. Chem. Soc.* **2007**, *129*, 3754–3762.
(36) Zana, R.; Benrraou, M.; Rueff, R. *Langmuir* **1991**, *7*, 1072–1075.
(37) Zhu, B. Y.; Zhao, G. X. *Huaxue Tongbao* **1981**, *6*, 21–26.
(38) Fan, Y.; Li, Y.; Yuan, G.; Wang, Y.; Wang, J.; Han, C. C.; Yan, H.; Li, Z.; Thomas, R. K. *Langmuir* **2005**, *21*, 3814–3820.
(39) Hao, J.; Wang, H.; Shi, S.; Lu, R.; Wang, T.; Li, G.; Sun, H. *Sci. China, Ser. B: Chem.* **1997**, *40*, 225–235.
(40) Hao, J.; Huang, J.; Xu, G.; Zheng, L.; Liu, W.; Hoffmann., H. *Sci. China, Ser. B: Chem.* **2003**, *46*, 567–576.
(41) Wang, X.; Li, Y.; Li, J.; Wang, J.; Wang, Y.; Guo, Z.; Yan, H. *J. Phys. Chem. B* **2005**, *109*, 10807–10812.
(42) Claessens, M. M. A. E.; Leermakers, F. A. M.; Hoekstra, F. A.; Stuart, M. A. C. *Langmuir* **2007**, *23*, 6315–6320.
(43) Nascimento, D. B.; Rapuano, R.; Lessa, M. M.; Carmona-Ribeiro, A. M. *Langmuir* **1998**, *14*, 7387–7391.
(44) Jiang, N.; Li, P.; Wang, Y.; Wang, J.; Yan, H.; Thomas, R. K. *J. Phys. Chem. B* **2004**, *108*, 15385–15391.
(45) Tata, M.; John, V. T.; Waguespack, Y. Y.; McPherson, G. L. *J. Phys. Chem.* **1994**, *98*, 3809–3817.
(46) Rizvi, S. A. A.; Shi, L.; Lundberg, D.; Menger, F. M. *Langmuir* **2008**, *24*, 673–677.
(47) Kabir-ud-Din Kumar, S.; Sharma, D. *J. Surfactants Deterg.* **2002**, *5*, 131–134.
(48) Han, F.; He, X.; Huang, J.; Li, Z.; Wang, Y.; Fu, H. *J. Phys. Chem. B* **2004**, *108*, 5256–5262.
(49) Elizalde, F.; Gracia, J.; Costas, M. *J. Phys. Chem.* **1988**, *92*, 3565–3568.

JP106031D